Brief Articles

Structural and Energetic Analyses of the Effects of the K103N Mutation of HIV-1 Reverse Transcriptase on Efavirenz Analogues

Marina Udier-Blagović, Julian Tirado-Rives, and William L. Jorgensen*

Department of Chemistry, Yale University, New Haven, Connecticut 06520-8107

Received July 18, 2003

The effect of the K103N mutation of HIV-1 reverse transcriptase (RT) on the activity of efavirenz analogues was studied via Monte Carlo/free energy perturbation calculations. The relative fold resistance energies indicate that efavirenz binds to K103N RT in a manner similar to the wild-type enzyme. The improved performance of the quinazolinones against the mutant enzyme is attributed to formation of a more optimal hydrogen-bonding network with bridging water molecules between the ligands and Glu138.

Introduction

Non-nucleoside inhibitors (NNRTIs) of HIV-1 reverse transcriptase (RT) are an important part of current anti-HIV therapy because of their diversity and specificity in targeting this enzyme, which is critical for viral replication. However, the efficacy of NNRTIs is seriously compromised by the emergence of mutant viral strains.[1,2] Some mutations, most notably K103N, are selected both in vitro and in vivo by most currently available NNRTIs.[3] K103N is also the most frequently observed mutation among patients failing highly active antiretroviral therapy (HAART) because it confers resistance to all of the clinically approved NNRTIs. Understanding the structural reasons behind variations in drug efficacy against viral mutants can contribute to the design of more effective therapeutic agents.

In this vein, a structural uncertainty has arisen concerning efavirenz, the current FDA-approved NNRTI with the best resistance profile. Two qualitatively different structures of its complex with K103N RT have been reported, and they lead to different explanations for the mutant's deleterious effect on the drug's potency.[4,5] The structure determined by Lindberg et al. (PDB code 1ikv) displays only minor positional variations for the protein side chains compared to the complex with wild-type (WT) RT,[4] while the structure from Ren et al. (PDB code 1fko) shows substantial deviations for three residues, Y181, E138, and K101 (Figure 1).[5] The most significant difference is for the orientation of Y181, which assumes the usual "up" position in the complexes with WT RT and in the 1ikv structure but adopts the uncommon "down" orientation in the 1fko complex. Only 3 of 47 NNRTI-RT complexes deposited in the PDB display the "down" orientation (PDB codes 1rti, 1fko, and 1rt3).[6] To further examine this issue, Monte Carlo/free energy perturbation (MC/FEP)[7] calculations were performed starting from the alternative crystal structures to (a) determine which complex leads to better agreement with the biological activity data, (b) gain insights into the structural origins of resistance caused by this mutation, and (c) obtain structural insights into the improved resistance profiles for quinazolinone analogues of efavirenz.

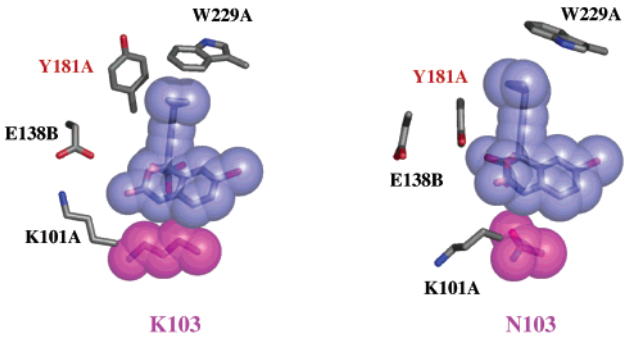

Figure 1. Efavirenz bound to wild-type RT (left) and K103N RT (right). Coordinates from ref 5 with the mutated residue 103 in magenta.

Computational Details

MC/FEP simulations were performed utilizing binding-site models derived from the 1ikv[4,8] and 1fko[5] crystal structures for efavirenz/K103N RT together with standard simulation protocols to predict relative fold resistance energies for efavirenz and two quinazolinone analogues, DPC961 and DPC083 (Scheme 1). The three compounds all have IC_{90} values of ca. 2 nM against WT RT in a cell-based assay.[9−12] However, efavirenz loses a factor of 38 (or 208)[4] in activity against the K103N mutant compared to WT RT, while the reductions are factors of 13 for DPC083 and 5 for DPC961.[9,10] DPC083 displays good pharmacological properties and is progressing in clinical trials.[13,14]

The binding-site models include the inhibitor and the nearest 123 protein residues. The initial conformations for the quinazolinones bound to WT and K103N RT were generated using the BOMB program.[15] Each protein−ligand complex was energy-minimized prior to the MC simulations using a distance-dependent dielectric constant of 4 ($\epsilon = 4r$) with the MCPRO program.[16] The energetics are described by the OPLS-AA force field except that CM1A atomic charges scaled by 1.14 are used for the inhibitors.[17] Full details of the MC simulation protocols are described elsewhere.[18,19]

* To whom correspondence should be addressed. Phone: 203 432-6278. Fax: 203 432-6299. E-mail: william.jorgensen@yale.edu.

10.1021/jm0303507 CCC: $27.50
Published on Web 03/20/2004

Scheme 1

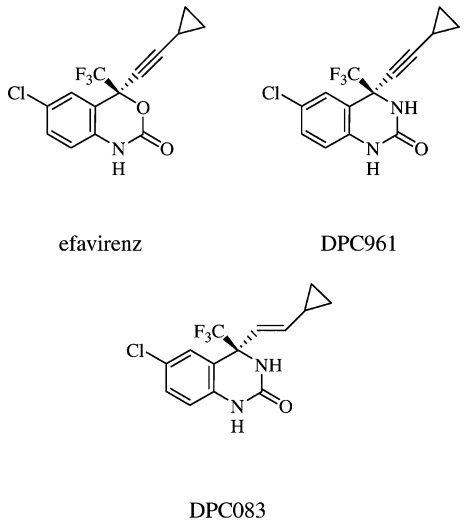

Scheme 2

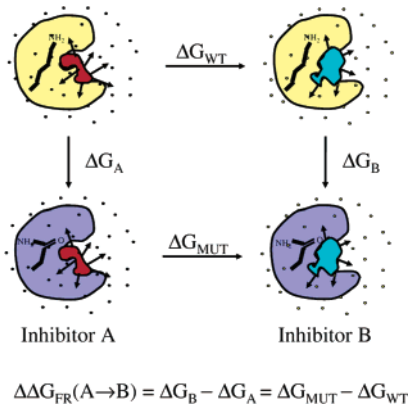

$$\Delta\Delta G_{FR}(A\rightarrow B) = \Delta G_B - \Delta G_A = \Delta G_{MUT} - \Delta G_{WT}$$

FEP calculations use the Zwanzig equation to compute the free energy change between two systems by converting one system to the other through a series of intermediate unphysical states.[20] To compute a relative fold resistance energy, $\Delta\Delta G_{FR}$, mutations of inhibitor **A** to inhibitor **B** can be performed, as illustrated in Scheme 2 (inhibitors **A** and **B** are red and cyan, while the WT and mutant protein are yellow and blue, respectively).

Specifically, inhibitor **A** is mutated to **B** while bound to the WT and mutant proteins, providing ΔG_{WT} and ΔG_{MUT}. Alternatively, mutation of the side chain for a residue, presently residue 103, can be performed to yield ΔG_A and ΔG_B. Normally, side chain perturbation is reserved for cases where the inhibitors exhibit large structural differences;[18,21,22] however, both pathways were considered here. $\Delta\Delta G_{FR}$ is then computed via $\Delta\Delta G_{FR} = \Delta G_{MUT} - \Delta G_{WT} = \Delta G_B - \Delta G_A$. The computed $\Delta\Delta G_{FR}$ represents the difference in the effects of the mutation on the free energies of binding for the two inhibitors. This is expected to parallel differences in the effects of the K103N mutation on the observed activities for **A** and **B** via

$$\Delta\Delta G_{FR} \approx RT(\ln IC_B^{N103}/IC_B^{K103} - \ln IC_A^{N103}/IC_A^{K103}) \quad (1)$$

The double-perturbation approach is particularly beneficial because potential issues associated with the cell-based assays such as cell penetration are expected to cancel out.

Each complex was solvated with a 22 Å water cap containing 851 TIP4P water molecules.[23] For the perturbations of the inhibitors, the FEP calculations utilized 10 windows with double-wide sampling resulting in a total of 20 free energy increments. Each MC simulation for a window covered 10M configurations of equilibration and 20M configurations of averaging. Perturbation of a side chain that involves a net change in charge, as in the present case, requires the use of a large number of intermediate states for good convergence. Thus, the number of windows was increased to 20 and the sampling periods were extended to 25M and 40M configurations, respectively.

Table 1. Fold Resistance Energies (kcal/mol) for K103N RT Relative to Efavirenz

	$\Delta\Delta G_{exp}$ [a]	$\Delta\Delta G_{calc}$ [b]	
		1fko	1ikv
efavirenz	0.00	0.00	0.00
DPC083	−0.66 ± 0.9	2.49 ± 0.22	−2.20 ± 0.29
DPC961	−1.25 ± 0.9	0.52 ± 0.18	−2.10 ± 0.28

[a] $\Delta G_{exp} \approx RT$ ln(activity) in kcal/mol. $\Delta\Delta G_{exp}$ is computed by taking the difference in ΔG_{exp} for two inhibitors. Experimentally determined anti-HIV activities are from refs 9−12. [b] $\Delta\Delta G_{calc}$ is computed using the thermodynamic cycle in Scheme 2. Statistical uncertainties are from the batch means procedure.

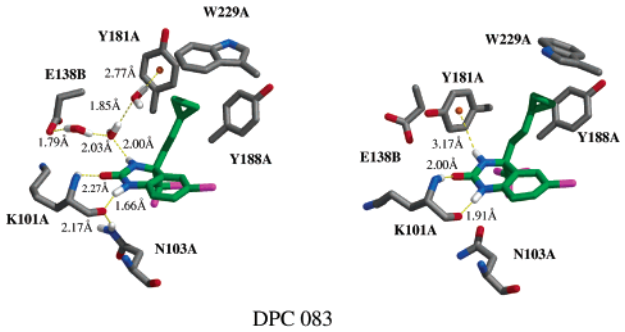

Figure 2. Computed structures from the MC simulations for DPC083 bound to 1ikv (left) and 1fko (right) K103N RT. Indicated distances are averaged over the MC simulations.

Results and Discussion

For the perturbations of the inhibitors, efavirenz was converted to DPC083 and DPC961 while bound to WT and K103N RT. The computed results starting from the 1ikv coordinates are in qualitative agreement with the experimental anti-HIV activities, while the computed $\Delta\Delta G_{FR}$ values from the complex with the uncommon Y181 orientation are inconsistent with the assay results (Table 1). The signs for the $\Delta\Delta G_{FR}$ should be negative to reflect that DPC083 and DPC961 are less adversely affected by the Lys103 to Asn substitution than efavirenz.[9−12] For example, note that the $\Delta\Delta G_{exp}$ for DPC961 comes from $RT(\ln 5 - \ln 38) = -1.25$ kcal/mol, while if the K103/N103 ratio of 208 is used for efavirenz,[4] the $\Delta\Delta G_{exp}$ for DPC083 and DPC961 would be further reduced to −1.71 and −2.30 kcal/mol. Explanations for the preference for the 1ikv-based structures are also suggested when the environments around the ligands are considered (Figure 2). Starting from the 1ikv structure, the MC simulations place two or three water molecules within 3 Å of the ligands to yield hydrogen-bonding networks in the vicinity of E138 and Y181. On the other hand, starting from the 1fko complex, these hydrogen-bonding networks are lost and the only replacement is an N−H···π interaction between one of the amido hydrogens of the quinazolinones and the aromatic ring of Y181.

FEP calculations were also performed starting from the WT structure[18] in which the side chain of residue 103 was perturbed from Lys to Asn in the presence of each inhibitor. The resultant computed $\Delta\Delta G_{FR}$ values between efavirenz and DPC083 and DPC961 are −1.2

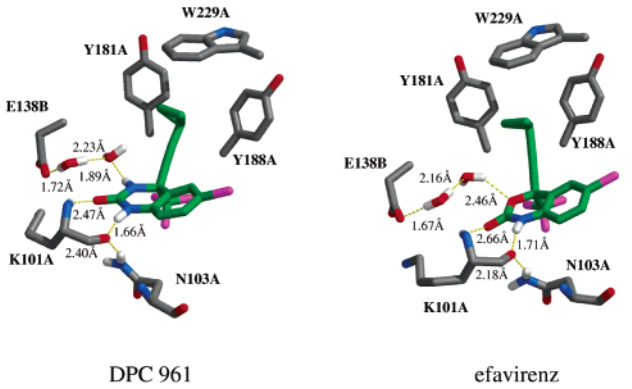

Figure 3. Computed structures for DPC961 and efavirenz bound to K103N RT. Indicated distances are averaged over the MC simulations.

± 0.4 and −3.5 ± 0.4 kcal/mol.[24] Although this side chain perturbation is computationally challenging, the resulting $\Delta\Delta G_{FR}$ values are qualitatively consistent with the FEP results for the ligand mutations starting from the 1ikv structure. In all, the present FEP results support the validity of the conventional orientation of Y181 for both the WT and K103N mutant protein in complex with efavirenz and the quinazolinones. Conventional RT structures were also found in the X-ray studies for the complexes of K103N RT with loviride and HBY 097.[25] It is suspected that specific crystallization conditions can lead to structures that are not fully representative of complexes in intracellular environments and/or under assay conditions. In particular, Ren et al.[5] state that they used a procedure to grow the crystals in a buffer at pH 5.0,[26] while the pH was near 7 for the crystallizations in refs 4 and 25 and for the assay work.[9−12] Though the Y181 down orientation is also unusual for RT structures from Ren and coworkers, use of low-pH conditions could lead to protonation of some carboxylate groups and salt-bridge disruption, e.g., for E138 and the K101-E138 salt bridge (Figure 1, right). In turn, such changes for the intraprotein hydrogen bonding could lead to other conformational adjustments, e.g., for the side chain of Y181. Packing differences can also arise from different crystallization conditions, though they have not been noted by the crystallographers in this case.[4,5] Systematic experimental study of the effects of crystallization conditions on structures for RT complexes would be most interesting.

The effect of the K103N mutation on the potency of efavirenz and other NNRTIs has been attributed to the loss of favorable hydrophobic interactions with the lysine side chain (Figure 1)[4] and to the ability of the mutated asparagine residue to stabilize the unliganded RT structure via hydrogen bonding to the Y188 side chain.[5,25] On the basis of the present structural results and those for a total of 47 efavirenz analogues,[27] an alternative contributor to the diminished potency of efavirenz analogues against the K103N mutant protein can be suggested (Figure 3). Electrostatic repulsion between the amido Hδ2 hydrogen of N103 and the amido hydrogen of the ligand's heterocyclic ring results in reduction of favorable interactions between the ligand and the mutant RT, as anticipated in the work of Lindberg et al.[4] Both hydrogens are hydrogen-bonding with the backbone carbonyl of K101. The average distances between these two hydrogens in the efavirenz/103N-RT, DPC083/103N-RT, and DPC961/103N-RT complexes from the MC simulations are only 2.04, 2.18, and 2.03 Å, respectively. Then an explanation for the superior potency of the quinazolinone analogues toward K103N RT can also be proposed. The presence of a more optimal water bridge between the additional amido hydrogen of the heterocyle and the side chain of E138 favors binding of DPC083 and DPC961 to K103N RT over the less ideal arrangement for efavirenz (Figures 2, left, and Figure 3). The computed average water H to oxazinone O distance of 2.46 Å is close to the typical upper limit of ca. 2.5 Å for hydrogen bonds.

Conclusions

The effect of the K103N mutation of HIV RT on the binding of efavirenz and the quinazolinone analogues DPC083 and DPC961 has been explored. The analogues display similar potency as efavirenz against WT RT but exhibit improved activity against this clinically important mutant enzyme. Computation of relative fold resistance energies between efavirenz and the two quinazolinones was performed by interconverting the ligands while bound to WT and K103N RT utilizing two structurally different efavirenz/K103N RT complexes as starting points. The computed results support the correctness of the structure of the K103N complex solved by Lindberg et al.,[4] which resembles most other complexes of NNRTIs with WT RT. Results of calculations performed starting from the coordinates of the alternative K103N structure with Y181, E138, and K101 shifted substantially from their positions for the WT complex do not agree with the experimental activity trends. The conclusions were further supported by FEP calculations for the K103N perturbation in the presence of all three inhibitors starting from the WT structure. The origin of diminished activity of the inhibitors against K103N RT was attributed in part to electrostatic repulsion between an amido hydrogen of the ligands and the Hδ2 hydrogen in the mutated asparagine. However, the improved potency of the quinazolinones compared to efavirenz may originate in the formation of a more optimal hydrogen-bonding network with water molecules between their additional amido hydrogen and the side chain of E138.

Acknowledgment. The authors thank Dr. Robert C. Rizzo for assistance, Drs. Cristiano R. W. Guimaraes and Steven S. Wesolowski for helpful discussions, and the National Institute of Allergy and Infectious Diseases (Grant AI44616) for financial support.

References

(1) De Clercq, E. New developments in anti-HIV chemotherapy. *Biochim. Biophys. Acta* **2002**, *1587*, 258−275.
(2) De Clercq, E. New anti-HIV agents and targets. *Med. Res. Rev.* **2002**, *22*, 531−565.
(3) Bacheler, L. T. Resistance to non-nucleoside inhibitors of HIV-1 reverse transcriptase. *Drug. Resist. Updates* **1999**, *2*, 56−67.
(4) Lindberg, J.; Sigurosson, S.; Löwgren, S.; Andersson, H. O.; Sahlberg, C.; Noreen, R.; Fridborg, K.; Zhang, H.; Unge, T. Structural basis for the inhibitory efficacy of efavirenz (DMP-266), MSC194 and PNU142721 towards the HIV-1 RT K103N mutant. *Eur. J. Biochem.* **2002**, *269*, 1670−1677.
(5) Ren, J.; Milton, J.; Weaver, K. L.; Short, S. A.; Stuart, D. I.; Stammers, D. K. Structural Basis for the Resilience of Efavirenz (DMP-266) to Drug Resistance Mutations in HIV-1 Reverse Transcriptase. *Structure* **2000**, *8*, 1089−1094.

(6) Berman, H. M.; Battistuz, T.; Bhat, T. N.; Bluhm, W. F.; Bourne, P. E.; Burkhardt, K.; Feng, Z.; Gilliland, G. L.; Iype, L.; Jain, S.; Fagan, P.; Marvin, J.; Padilla, D.; Ravichandran, V.; Schneider, B.; Thanki, N.; Weissig, H.; Westbrook, J. D.; Zardecki, C. The Protein Data Bank. *Acta Crystallogr., Sect. D: Biol. Crystallogr.* **2002**, *58*, 899−907.

(7) Jorgensen, W. L. Free Energy Changes in Solution. In *Encyclopedia of Computational Chemistry*; Schleyer, P. v. R., Allinger, N. L., Clark, T., Kollman, P. A., Schaefer, H. F., Schreiner, P. R., Eds.; Wiley: New York, 1998; pp 1061−1070.

(8) The position of N103 is undefined in this efavirenz/K103N RT complex. The missing residue was incorporated from the nevirapine/K103N RT structure (PDB code 1fkp) by overlying the backbone of residues Y188, Y181, K101, and W229 in both proteins. Since the electron density for the amide plane of N103 is not well defined, the efavirenz/K103N RT complex was subjected to 30 million configurations of equilibration in an MC simulation with explicit inclusion of water molecules. The equilibrated structure was then used as the starting point in all subsequent MC/FEP calculations.

(9) Corbett, J. W.; Ko, S. S.; Rodgers, J. D.; Gearhart, L. A.; Magnus, N. A.; Bacheler, L. T.; Diamond, S.; Jeffrey, S.; Klabe, R. M.; Cordova, B. C.; Garber, S.; Logue, K.; Trainor, G. L.; Anderson, P. S.; Erickson-Viitanen, S. K. Inhibition of clinically relevant mutant variants of HIV-1 by quinazolinone non-nucleoside reverse transcriptase inhibitors. *J. Med. Chem.* **2000**, *43*, 2019−2030.

(10) Corbett, J. W.; Pan, S.; Markwalder, J. A.; Cordova, B. C.; Klabe, R. M.; Garber, S.; Rodgers, J. D.; Erickson-Viitanen, S. K. 3,3a-Dihydropyrano[4,3,2-*de*]quinazolin-2(1*H*)-ones are potent non-nucleoside reverse transcriptase inhibitors. *Bioorg. Med. Chem. Lett.* **2001**, *11*, 211−214.

(11) Cocuzza, A. J.; Chidester, D. R.; Cordova, B. C.; Jeffrey, S.; Parsons, R. L.; Bacheler, L. T.; Erickson-Viitanen, S.; Trainor, G. L.; Ko, S. S. Synthesis and evaluation of efavirenz analogues as HIV-1 reverse transcriptase inhibitors: replacement of the cyclopropylacetylene side chain. *Bioorg. Med. Chem. Lett.* **2001**, *11*, 1177−1179.

(12) Cocuzza, A. J.; Chidester, D. R.; Cordova, B. C.; Klabe, R. M.; Jeffrey, S.; Diamond, S.; Weigelt, C. A.; Ko, S. S.; Bacheler, L. T.; Erickson-Viitanen, S. K.; Rodgers, J. D. 1,4-Benzoxazepinone analogues of efavirenz (Sustiva) as HIV-1 reverse transcriptase inhibitors. *Bioorg. Med. Chem. Lett.* **2001**, *11*, 1389−1392.

(13) Sorbera, L. A.; del Fresno, M.; Leeson, P. A.; Silvestre, J.; Rabasseda, X. DPC-083 Anti-HIV Reverse Transcriptase Inhibitor. *Drugs Future* **2002**, *27*, 331−338.

(14) Cohen, J. Special News Report: HIV/AIDS. *Science* **2002**, *296*, 2320−2324.

(15) Jorgensen, W. L. *BOMB* (formerly *GenMol*), version 2.1; Yale University: New Haven, CT, 2002.

(16) Jorgensen, W. L. *MCPRO*, version 1.68; Yale University: New Haven, CT, 2002.

(17) Udier-Blagović, M.; Jorgensen, W. L. Accuracy of Free Energies of Hydration for Organic Molecules from CM1 and CM3 Partial Atomic Charges. *J. Comput. Chem.* (in press).

(18) Rizzo, R. C.; Wang, D.; Tirado-Rives, J.; Jorgensen, W. L. Validation of a Model for the Complex of HIV-1 Reverse Transcriptase with Sustiva through Computation of Resistance Profiles. *J. Am. Chem. Soc.* **2000**, *122*, 12898−12900.

(19) Rizzo, R. C.; Udier-Blagović, M.; Wang, D.; Watkins, E. K.; Smith, M. B. K.; Smith, R. H. J.; Tirado-Rives, J.; Jorgensen, W. L. Prediction of Activity for Non-nucleoside Inhibitors with HIV-1 Reverse Transcriptase Based on Monte Carlo Simulations. *J. Med. Chem.* **2002**, *45*, 2970−2987.

(20) Zwanzig, R. W. High-Temperature Equation of State by a Perturbation Method. I. Nonpolar Gases. *J. Chem. Phys.* **1954**, *22*, 1420−1426.

(21) Wang, D.; Rizzo, R. C.; Tirado-Rives, J.; Jorgensen, W. L. Antiviral Drug Design: Computational Analyses of the Effects of the L100I Mutation for HIV-RT on the Binding of NNRTIs. *Bioorg. Med. Chem. Lett.* **2001**, *11*, 2799−2802.

(22) Udier-Blagović, M.; Tirado-Rives, J.; Jorgensen, W. L. Validation of a Model for the Complex of HIV-1 Reverse Transcriptase with Nonnucleoside Inhibitor TMC125. *J. Am. Chem. Soc.* **2003**, *125*, 6016−6017.

(23) Jorgensen, W. L.; Chandrasekhar, J.; Madura, J. D.; Impey, R. W.; Klein, M. L. Comparison of simple potential functions for simulating liquid water. *J. Chem. Phys.* **1983**, *79*, 926−935.

(24) The FEP calculations involving mutation of the side chain were performed utilizing 1.08 × CM1A charges for the inhibitors, consistent with prior MC/FEP and MC/ELR calculations, e.g. refs 18 and 19. The scaling factor of 1.14 was adopted after a recent demonstration that it improves predictions for free energies of hydration of organic molecules. For additional details, see ref 17.

(25) Hsiou, Y.; Ding, J.; Das, K.; Clark, A. D., Jr.; Boyer, P. L.; Lewi, P.; Janssen, P. A.; Kleim, J. P.; Rosner, M.; Hughes, S. H.; Arnold, E. The Lys103Asn mutation of HIV-1 RT: a novel mechanism of drug resistance. *J. Mol. Biol.* **2001**, *309*, 437−445.

(26) Stammers, D. K.; Somers, D. O'N.; Ross, C. K.; Kirby, I.; Ray, P. H.; Wilson, J. E.; Norman, M.; Ren, J. S.; Esnouf, R. M.; Garman, E. F.; Jones, E. Y.; Stuart, D. I. Crystals of HIV-1 Reverse Transcriptase Diffracting to 2.2 Å Resolution. *J. Mol. Biol.* **1994**, *242*, 586−588.

(27) Udier-Blagović, M.; Watkins, E. K.; Tirado-Rives, J.; Jorgensen, W. L. Activity Predictions for Efavirenz Analogues with the K103N Mutant of HIV Reverse Transcriptase. *Bioorg. Med. Chem. Lett.* **2003**, *13*, 3337−3340.

JM0303507